Mechanism of Inhibition of Cyclic Nucleotide–gated Ion Channels by Diacylglycerol

JENNIFER I. CRARY, DYLAN M. DEAN, WANG NGUITRAGOOL, PERI T. KURSHAN, and ANITA L. ZIMMERMAN

From the Department of Molecular Pharmacology, Physiology and Biotechnology, Brown University, Providence, Rhode Island 02912

ABSTRACT Cyclic nucleotide–gated (CNG) channels are critical components in the visual and olfactory signal transduction pathways, and they primarily gate in response to changes in the cytoplasmic concentration of cyclic nucleotides. We previously found that the ability of the native rod CNG channel to be opened by cGMP was markedly inhibited by analogues of diacylglycerol (DAG) without a phosphorylation reaction (Gordon, S.E., J. Downing-Park, B. Tam, and A.L. Zimmerman. 1995. *Biophys. J.* 69:409–417). Here, we have studied cloned bovine rod and rat olfactory CNG channels expressed in *Xenopus* oocytes, and have determined that they are differentially inhibited by DAG. At saturating [cGMP], DAG inhibition of homomultimeric (α subunit only) rod channels was similar to that of the native rod CNG channel, but DAG was much less effective at inhibiting the homomultimeric olfactory channel, producing only partial inhibition even at high [DAG]. However, at low open probability (P_o), both channels were more sensitive to DAG, suggesting that DAG is a closed state inhibitor. The Hill coefficients for DAG inhibition were often greater than one, suggesting that more than one DAG molecule is required for effective inhibition of a channel. In single-channel recordings, DAG decreased the P_o but not the single-channel conductance. Results with chimeras of rod and olfactory channels suggest that the differences in DAG inhibition correlate more with differences in the transmembrane segments and their attached loops than with differences in the amino and carboxyl termini. Our results are consistent with a model in which multiple DAG molecules stabilize the closed state(s) of a CNG channel by binding directly to the channel and/or by altering bilayer–channel interactions. We speculate that if DAG interacts directly with the channel, it may insert into a putative hydrophobic crevice among the transmembrane domains of each subunit or at the hydrophobic interface between the channel and the bilayer.

KEY WORDS: rod • olfactory receptor • channel modulation • lipid bilayer • tetracaine

INTRODUCTION

Cyclic nucleotide–gated (CNG)[1] ion channels play a vital role in visual transduction (for review see Roof and Makino, 2000) and olfaction (for reviews see Dionne and Dubin, 1994; Zufall et al., 1994; Menini, 1995), and have been identified in numerous other tissues, including the heart (Biel et al., 1993; Ruiz et al., 1996) and kidney (Biel et al., 1994). CNG channels have been shown to consist of two to three (Bönigk et al., 1999) different types of subunits arranged in a tetrameric structure (for reviews see Kaupp, 1995; Molday and Hsu, 1995; Yau and Chen, 1995; Zimmerman, 1995; Finn et al., 1996; Zagotta and Siegelbaum, 1996; Wei et al., 1998; Broillet and Firestein, 1999). They are structurally homologous to voltage-gated ion channels (Jan and Jan, 1992) with six transmembrane segments and a pore-forming loop between S5 and S6, but they are only weakly voltage-activated, and they open in response to cyclic nucleotides whose concentration varies with physiological status. Most CNG channels, including rod and olfactory types, are non-selective cation channels whose opening causes membrane depolarization and Ca^{2+} entry (for reviews see Kaupp, 1995; Zimmerman, 1995).

In rod cells, light activates an enzyme cascade that decreases the level of cytosolic cGMP, resulting in the closure of CNG channels that are normally open in the dark (for review see Roof and Makino, 2000). In contrast, odorants activate another enzyme cascade that leads to the stimulation of adenylate cyclase and the production of cAMP, which opens olfactory CNG channels (for reviews see Dionne and Dubin, 1994; Zufall et al., 1994; Menini, 1995). Olfactory and rod CNG channels have similar properties, but olfactory channels are much more sensitive to cyclic nucleotides than are rod channels. Olfactory channels also respond to comparable concentrations of cAMP and cGMP, whereas rod channels are much more sensitive to cGMP than to cAMP (for reviews see Zimmerman, 1995; Zagotta and

Address correspondence to Anita L. Zimmerman, Department of Molecular Pharmacology, Physiology and Biotechnology, Box G-B329, Brown University, Providence, RI 02912. Fax: (401) 863-1222; E-mail: anita_zimmerman@brown.edu

[1]*Abbreviations used in this paper:* CNG, cyclic nucleotide–gated; DAG, diacylglycerol; P_o, open probability.

Siegelbaum, 1996). In fact, cAMP is only a partial agonist of the rod CNG channels. Furthermore, CNG channels are modulated by cellular factors, including phosphorylation enzymes (Gordon et al., 1992; Molokanova et al., 1997; Muller et al., 1998), Ca^{2+}/calmodulin (Hsu and Molday, 1993; Chen and Yau, 1994; Gordon et al., 1995b), endogenous Ca^{2+} binding proteins (Gordon et al., 1995b; Balasubramanian et al., 1996), transition metal divalent cations (Idelfonse et al., 1992; Karpen et al., 1993; Gordon and Zagotta, 1995a), and lipids, including diacylglycerol (DAG; Gordon et al., 1995a; Womack et al., 2000).

We previously reported that DAG modulation of the native CNG channel from frog rod outer segments is independent of phosphorylation (Gordon et al., 1995a). Evidence suggests that DAG also modulates other types of ion channels independently of protein kinase C, causing either activation or inhibition of channel function (Bowlby and Levitan, 1995; Hofmann et al., 1999). In addition, DAG is a potential precursor of polyunsaturated fatty acids, such as arachidonic and linoleic acids, both of which have been shown to reversibly activate light-sensitive channels in *Drosophila* photoreceptors (Chyb et al., 1999). Thus, the production of DAG via activation of phospholipase C may have multiple ways of affecting channel behavior without relying on a phosphorylation pathway. Interestingly, a recent study of mammalian rod CNG channels (α and β subunits) expressed in *Xenopus* oocytes has shown that long-chain DAG is stimulatory, whereas the cellular precursor to DAG, PIP_2, is inhibitory. However, PIP_2 inhibition is not as strong when only α subunits are expressed (Womack et al., 2000). Although a physiological role for DAG in the visual or olfactory pathway remains undetermined, in the present study, DAG is used as a tool to dissect the functional differences of the rod and olfactory CNG ion channels.

To elucidate the mechanism of DAG inhibition of CNG channels, we explored the effect of a short-chain DAG analogue on cloned rod and olfactory channels expressed in *Xenopus* oocytes. Rod channels exhibited greater inhibition than olfactory channels at saturating cGMP concentrations. However, DAG inhibition was much more efficient at low open probabilities for both channel types, suggesting that DAG stabilizes the closed states of the channel. In addition, the Hill coefficients from DAG dose–response curves suggested that multiple DAG molecules participate in the inhibition of a channel.

Because these two CNG channels showed differences in their inhibition by DAG, we also examined the DAG modulation of a series of chimeras of the rod and olfactory channels (Gordon and Zagotta, 1995b; Fodor et al., 1997). Our findings suggest that the sequence differences in the transmembrane segments and loop structures, rather than those in the amino and carboxyl termini, may be responsible for the differences in DAG inhibition between the two channels. At saturating cGMP, Hill coefficients for DAG inhibition ranged from 1.5 to 2.8 for this series of chimeras, indicating that its mechanism of inhibition must differ from that of tetracaine, which demonstrates a Hill coefficient of ∼1 and shows obvious voltage dependence (Fodor et al., 1997). We propose that DAG stabilizes the closed states of the channels either by direct interaction with the channel protein, by distortion of bilayer–channel interactions, or by some combination of these mechanisms.

MATERIALS AND METHODS

Expression of Channels in Xenopus Oocytes

The plasmids containing the α subunits of bovine rod (CNG1), rat olfactory (CNG2), and chimeric cDNA were provided by William N. Zagotta (University of Washington, Seattle, WA). See Richards and Gordon (2000) for other terminology for these channels. The olfactory α subunit clone originated from the laboratories of R.R. Reed (Johns Hopkins University, Baltimore, MD) and R.S. Molday (University of British Columbia, Vancouver, British Columbia, Canada). Construction of the chimeras was previously described in Gordon and Zagotta (1995b). The plasmid containing the mouse olfactory clone was provided by Maria Ruiz (Entelos, Inc., Menlo Park, CA) (Ruiz et al., 1996), and this channel has been shown to behave similarly to the rat olfactory channel (Crary et al., 2000); in this study, the wild-type mouse olfactory channel was only used for the single-channel analysis. The vectors all contain the untranslated sequence of the *Xenopus* β-globin gene, which promotes high protein expression in oocytes (Liman et al., 1992). Capped cRNA was made by in vitro transcription using either Promega's RiboMAX™ large-scale RNA production system or Ambion's mMessage Machine.

Sections of ovaries containing oocytes were surgically removed from anesthetized *Xenopus laevis* frogs, and individual oocytes were isolated from clumps of tissue by treatment with 1 mg/ml collagenase type 1A (Sigma-Aldrich) in a buffer containing low calcium (82.5 mM NaCl, 2.5 mM KCl, 5 mM HEPES, and 1 mM $MgCl_2$, pH 7.6). The cRNA was injected into *Xenopus* oocytes using a Drummond Nanoject oocyte injector. The injected oocytes were initially incubated at 15°C overnight, and then at 18°C for 1–10 d before testing for expression via the patch-clamp technique. For single channel studies, the oocytes were stored at 4°C once a desirable level of expression was reached. The saline solution for maintaining oocytes contained the following: 96 mM NaCl, 2 mM KCl, 1.8 mM $CaCl_2$, 5 mM HEPES, 1 mM $MgCl_2$, 2.5 mM pyruvic acid, 100 U/ml penicillin, and 100 μg/ml streptomycin, pH 7.6. The vitelline membrane was removed by treatment with a hypertonic solution (200 mM *N*-methyl-D-glucamine, 2 mM KCl, 10 mM EGTA, 10 mM HEPES, and 1 mM $MgCl_2$, pH 7.4) and mechanical dissection to expose the plasma membrane for patch-clamp recording.

Application of Electrophysiological Solutions

The oocyte chamber for patch-clamp experiments was a plastic petri dish, and water-soluble solutions were applied using a 36-solution patch perfusion system, the RSC-100 rapid solution changer (Molecular Kinetics). Solutions consisted of the following: 130 mM NaCl, 0.2 mM EDTA, and 2 mM HEPES buffer, pH 7.2, with varying concentrations of cGMP (Sigma-Aldrich) and

cAMP (Calbiochem-Novabiochem). When necessary, 500 μM niflumic acid (Sigma-Aldrich) was added to the extracellular solution to block Ca^{2+}-activated Cl^- channels, which are endogenous to the oocyte membranes. The DAG analogue, 1,2-dioctanoyl-*sn*-glycerol (1,2-DiC8; Sigma-Aldrich) was dissolved in DMSO (Sigma-Aldrich) at 0.5–20-mM stock concentrations and stored at −20°C. Because of the lipophilicity of the analogues, the DAG solutions were not applied to the patch through Teflon tubing because we found that this resulted in a decrease in the response, as though the DAG had adhered to the tubing, effectively reducing the concentration of the DAG before its exposure to the patch. Instead, the DAG analogue was applied to the intracellular surfaces of patches by direct addition to the bathing solution in the petri dish, where it was carefully and thoroughly mixed using a transfer pipet. The petri dish and agar bridge were replaced after each experiment with DAG.

Electrophysiological Recordings and Analysis

Data were collected from inside-out patches in the steady state after any spontaneous changes in cGMP affinity, which usually resulted in a left shift of the cGMP dose–response curve. These changes have been attributed to dephosphorylation by endogenous patch-affiliated phosphatases (Gordon et al., 1992; Molokanova et al., 1997), and were monitored here by sampling the current periodically at a low level of cGMP (below the $K_{1/2}$) while incubating the patch in saturating cGMP and waiting for the monitored current to stabilize. The time required for this stabilization ranged from ∼10 to 40 min, and the magnitude and time course of the effect varied with the channel type.

For DAG dose–response curves, the bath contained a saturating concentration of cGMP (2 mM for rod and chimeric channels and 100 μM for olfactory), and DAG was added in increments resulting in changes in bath concentration ranging from 0.05 to 48 μM. However, the DMSO concentration remained below 1.2%, which had no effect on the channels or the leak current. The current was monitored for several minutes after each addition of DAG to insure that the effect of the DAG had stabilized; stabilization was usually complete within <1 or 2 min. This time may have been required for DAG to insert into the membrane, and the reversal of the DAG effect was also slow as reported previously (Gordon et al., 1995a). Although we cannot measure the final concentration of DAG in the membrane after this stabilization, we were working well below the critical micelle concentration (270 μM) of a similar hydrophobic molecule (1,2-dioctanoyl phosphatidylcholine; Marsh and Phil, 1990) and below the IC_{50} reported for DAG inhibition of peptide-induced polarity of neutrophils (Zimmermann et al., 1988), indicating that we are in the linear concentration range during our DAG dose–response experiments. In fact, the DAG dose–response curve for CHM3 provides evidence that the concentration of DAG is increasing incrementally up to at least 6 μM (see Fig. 7), confirming the availability of soluble DAG for the observed partial response of the olfactory channel in this same range.

For experiments with the native channel, rod cells were obtained from *Rana Pipiens* according to an established method (Zimmerman and Baylor, 1992). Excised inside-out patches from rod outer segments were studied using the same methods and solutions as for the *Xenopus* oocytes. Pipet openings were 0.5–20 μm in diameter and had resistances of 0.6–15 MΩ. All recordings were obtained at room temperature (20–25°C). Recordings of the current were made as the voltage was changed from −100 to +100 mV in steps of 20 or 50 mV, from a holding potential of 0 mV. The leak currents obtained in the absence of cGMP were subtracted from each record. For single-channel studies, three to five continuous 1-s recordings were made at +80 mV.

Sampling (digitization) of currents was accomplished using an Axopatch 1B, 1C, or 200 patch-clamp amplifier (Axon Instruments) with analogue-to-digital converters, which sent output to a Macintosh Quadra computer running Pulse software (Instrutech). Before digitization, the data were low pass–filtered using a selectable 8-pole Bessel filter (Frequency Devices). The filter cutoff frequency (−3 dB point) was 2 kHz for multichannel patches and 5 kHz for single-channel patches. Sampling rates were set at five times the filter cutoff frequency to prevent aliasing. Data analysis was performed with the graphical analysis software IgorPro (WaveMetrics).
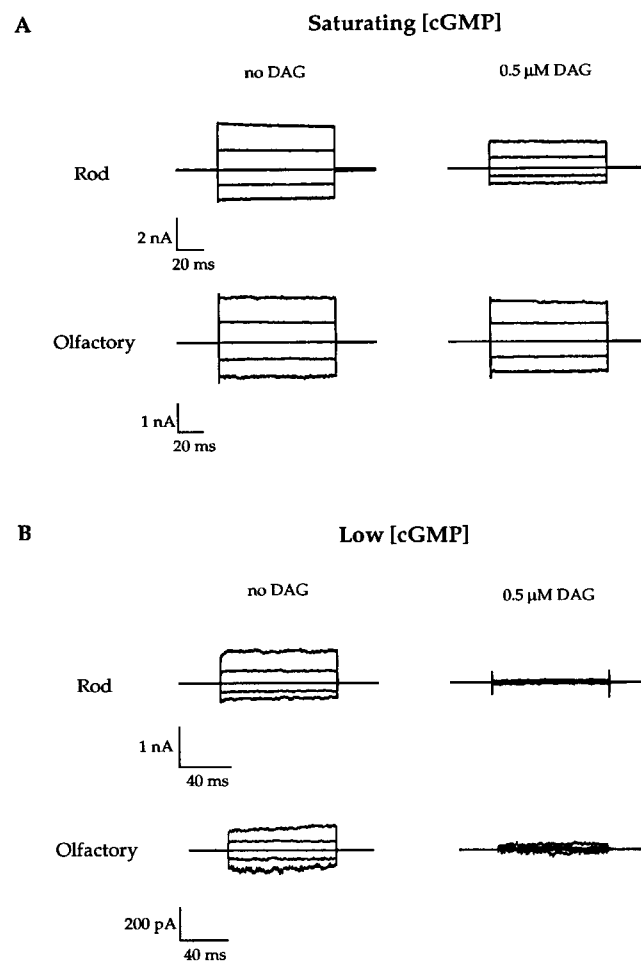

FIGURE 1. Inhibition by DAG is more pronounced for rod than for olfactory CNG channels. Data were measured from multichannel, inside-out patches of homomultimeric (α only) rod and olfactory channels. The families of cGMP-activated currents were recorded in response to voltage jumps ranging from −100 to +100 mV in steps of 50 mV, from a holding potential of 0 mV. Currents measured in the absence of cGMP were subtracted from all traces. 2 mM cGMP and 100 μM cGMP are saturating levels of cGMP for rod and olfactory channels, respectively. (A) Inhibition at saturating cGMP: rod channels, 42% inhibition; and olfactory channels, 10% inhibition. (B) Inhibition at low cGMP concentrations: rod channels, 10 μM cGMP, I/I_{max} = 0.2 before DAG application, and 93% inhibition by DAG; olfactory channels, 2 μM cGMP, I/I_{max} = 0.6 before DAG application, and 72% inhibition by DAG.

DAG Inhibition of Rod Channels Is Greater than that of Olfactory Channels

Fig. 1 demonstrates that DAG has a greater inhibitory effect on rod channels than on olfactory channels and that both channel types are more sensitive to DAG at low concentrations of agonist. Electrophysiological recordings were obtained from inside-out excised patches from *Xenopus* oocytes expressing α homomultimers of bovine rod or rat olfactory CNG ion channels. Fig. 1 shows the current traces recorded for each wild-type channel at low and high cGMP concentrations in both the presence and absence of 0.5 μM DAG. At saturating cGMP concentrations, this low dose of DAG had a small effect on the olfactory channel, but decreased the current of the rod channel by ~42%. At lower cGMP concentrations (near the $K_{1/2}$ for each channel), the same amount of DAG reduced the current for both rod and olfactory channels to a greater extent. This suppression was found to be reversible (data not shown), which is consistent with the reversible suppression observed for the native rod channels (Gordon et al., 1995a). Furthermore, this inhibition by DAG occurred in the absence of ATP, demonstrating that DAG cannot be acting through phosphorylation by protein kinase C. In addition, consistent with the original study (Gordon et al., 1995a), 1,3-DiC8 was just as effective as 1,2-DiC8, and 1,2-dioctanoyl ethylene glycol was much less effective (data not shown).

Fig. 2 illustrates a more quantitative comparison of the response of the two channels to DAG. Dose–response curves for activation of each channel by cGMP demonstrate a large shift to the right in the presence of 0.5 μM DAG. For the rod channel, the $K_{1/2}$ increased by a factor of 3.2, from 24 to 76 μM cGMP, and for the olfactory channel, the $K_{1/2}$ increased by a factor of 2.2, from 1.8 to 4.0 μM cGMP. For the rod channel, there is also a significant (29%) reduction in the maximal current with DAG, whereas this reduction is much smaller (3%) for the olfactory channel. The Hill coefficients remained essentially unchanged for both channels.

Previous results showed that application of excess cyclic nucleotide did not reverse the inhibition of the native rod channel by DAG, suggesting that the lower apparent affinity does not result from competitive inhibition of agonist binding (Gordon et al., 1995a). Similar findings in the current study suggest that this is also the case for the cloned channels. This is apparent for the rod channel in Fig. 2 A: increasing [cGMP] beyond saturation does not induce recovery of the DAG-suppressed current. A similar result was observed with the olfactory channel when a higher DAG concentration was used to produce a greater decrease in maximal current at high cGMP concentrations (data not shown).
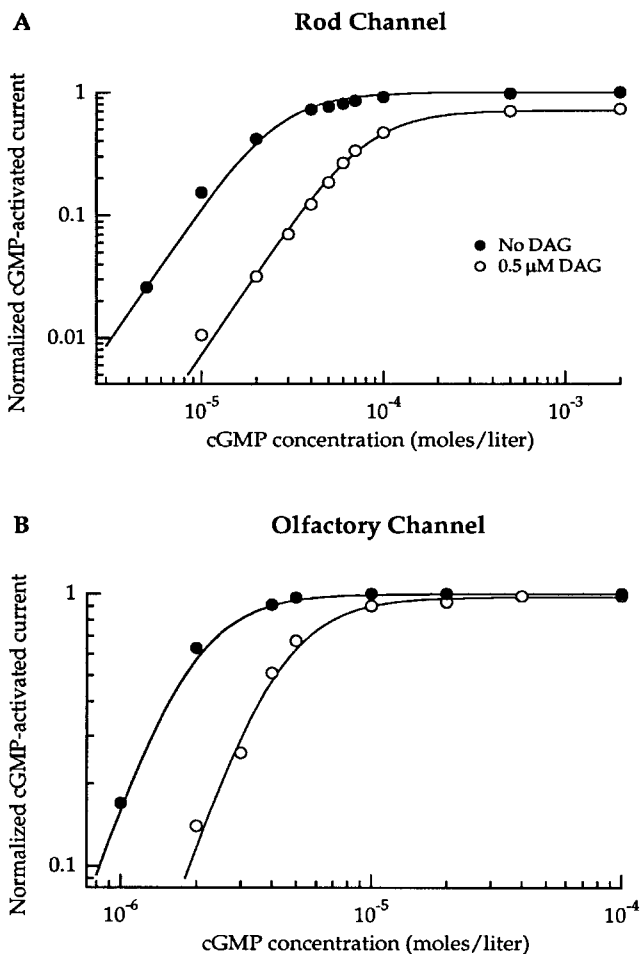

A Rod Channel

B Olfactory Channel

FIGURE 2. Dose–response curves for rod and olfactory channels demonstrate differential inhibition by DAG. Bath contained low divalent NaCl solution with or without 0.5 μM DAG and various concentrations of cGMP. Steady-state, cGMP-activated currents were measured at +100 mV from a single patch containing either rod or olfactory channels and were normalized to the I_{max} without DAG. Smooth curves were drawn by fitting the averaged data with the Hill equation, $I/I_{max} = [cGMP]^n/(K_{1/2}^n + [cGMP]^n)$, where I is the cGMP-activated current, I_{max} is the cGMP-activated current obtained at saturating cGMP, $K_{1/2}$ is the concentration of cGMP giving half maximal activation, and n is the Hill coefficient. In fitting the data, this relation was scaled to match the measured maximal I/I_{max} (e.g., the maximal I/I_{max} for the rod channel in the presence of 0.5 μM DAG was only 0.71 here, rather than 1). The Hill relation was used only for an empirical description of the data to quantify changes in the apparent affinity and maximal activation (or inhibition; see Fig. 3); it is not meant to suggest a mechanism of channel activation or inhibition by DAG. (A) Rod channels. Top curve (without DAG): $I/I_{max} = 1$, n = 2.25, and $K_{1/2} = 24$ μM. Bottom curve (with DAG): $I/I_{max} = 0.71$, n = 2.25, and $K_{1/2} = 76$ μM. (B) Olfactory channels. Top curve (without DAG); $I/I_{max} = 1$, n = 2.8, and $K_{1/2} = 1.8$ μM. Bottom curve (with DAG): $I/I_{max} = 0.97$, n = 2.8, and $K_{1/2} = 4.0$ μM.

The dose–response curves for DAG at saturating [cGMP] are dramatically different for the rod and olfactory channels. Fig. 3 indicates that rod cGMP-activated currents are completely suppressed by ~3 μM

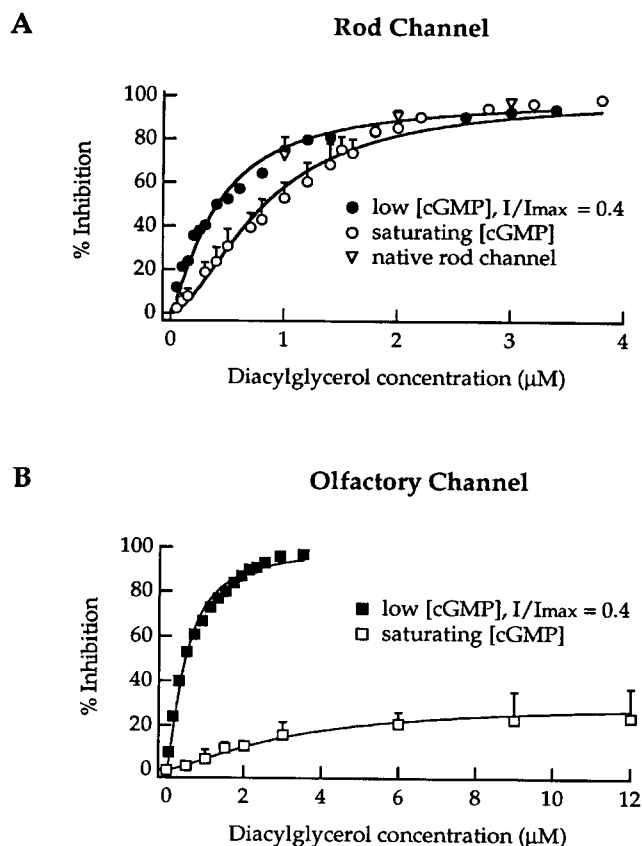**A**

Rod Channel

B

Olfactory Channel

FIGURE 3. Rod channel currents show complete suppression by DAG at saturating cGMP concentration, whereas olfactory channel currents show only partial suppression; inhibition by DAG is greater at low than at high cGMP concentration. Averaged data obtained at saturating cGMP were fit with the Hill equation, $IN/IN_{max} = [DAG]^n/(IC_{50}{}^n + [DAG]^n)$, where IN is percent inhibition, IN_{max} is maximal inhibition, IC_{50} is the concentration of DAG required to achieve half maximal inhibition, and n is the Hill coefficient. As for Fig. 2, the relation was scaled to reflect the measured maximal IN/IN_{max}. Data points at low cGMP are from a single rod or olfactory patch at a concentration of cGMP that gave ~40% of maximal current. This finding was consistent in several other patches of each type. Data points at saturating cGMP (2 mM for rod and 100 μM for olfactory) are averaged values, plotted with SD (error bars) of data from 11 patches for rod and 13 patches for olfactory channels. Note the different scales of the two figures. (A) Rod channels. (Closed circles) At ~30 μM cGMP, $IN_{max} = 100\%$, $IC_{50} = 0.41$ μM, and n = 1.3. (Open circles) At 2 mM cGMP, $IN_{max} = 100\%$, $IC_{50} = 0.83$ μM, and n = 1.7. Triangles represent data from native rod channels (two patches), included for comparison with the cloned channels. (B) Olfactory channels. (Closed squares) At 1.5 μM cGMP, $IN_{max} = 100\%$, $IC_{50} = 0.47$ μM, and n = 1.4. (Open squares) At 100 μM cGMP, $IN_{max} = 31\%$, $IC_{50} = 3.24$ μM, and n = 1.4.

DAG at saturating (2 mM) cGMP, but the olfactory cGMP-activated currents show only partial suppression at saturating (100 μM) cGMP, even with DAG concentrations as high as 12 μM. In fact, the fractional suppression of the olfactory channel remained at this low level even when we raised the DAG concentration to 48

μM (data not shown). For the rod channel, the IC_{50} for inhibition was 0.83 μM DAG, and the Hill coefficient was 1.7. However, for the olfactory channel, the concentration required to obtain half maximal inhibition was 3.24 μM DAG, with a Hill coefficient of 1.4. Thus, there is approximately a fourfold difference between the DAG IC_{50} obtained for the rod channel and that obtained for the olfactory channel at saturating [cGMP].

Fig. 3 also demonstrates the higher sensitivity of both channels to DAG at lower concentrations of cGMP. The DAG dose–response curve from a representative patch at low [cGMP] is shown for each channel. In comparison to the corresponding DAG dose–response curve at high [cGMP], the curve at low [cGMP] is shifted to the left for both channels, and, interestingly, for the olfactory channel, the inhibition reaches 100%. The I/I_{max} for both channels was ~0.40 before the addition of DAG; the IC_{50} values for inhibition were 0.41 and 0.47 μM, and the Hill coefficients were 1.3 and 1.4 for the rod and olfactory channels, respectively. Furthermore, for the rod channel, DAG inhibition at saturating [cAMP] was comparable to that at a low cGMP concentration that produced a similar fractional activation (data not shown). This finding suggests that DAG preferentially affects closed channels, regardless of ligand occupancy.

For the native rod channel, the DAG IC_{50} was previously reported to be 22 μM, which is quite different from the value reported here for the cloned rod homomultimer. Although preliminary studies with the cloned channel resulted in development of a new method of administering DAG to the patch without the use of Teflon (see MATERIALS AND METHODS), we could not ignore the possibility that the cloned channel might be more sensitive to the DAG analogue than is the native channel. Thus, we reexamined the native channel using our new DAG application technique. Our data confirmed that the response of the native channel to the DAG analogue is similar to that for the cloned channel, as shown by the triangles in Fig. 3. This indicates that the values from the previous study are in error, most likely because of the adherence of DAG to the Teflon delivery tubes, effectively reducing the concentration of DAG in solution.

Reductions in Maximal Current Are Due to Decreasing Open Probability

Single-channel analysis was performed to determine whether the reduction in the maximal current by DAG was due to a decrease in open probability (P_o) or in single-channel conductance. Figs. 4 and 5 show single-channel currents and amplitude histograms at +80 mV for rod and olfactory channels in the presence and absence of DAG. The patch in Fig. 4 contained two rod channels (see legend for note about sequence); the patch in Fig. 5 contained a single wild-type olfactory
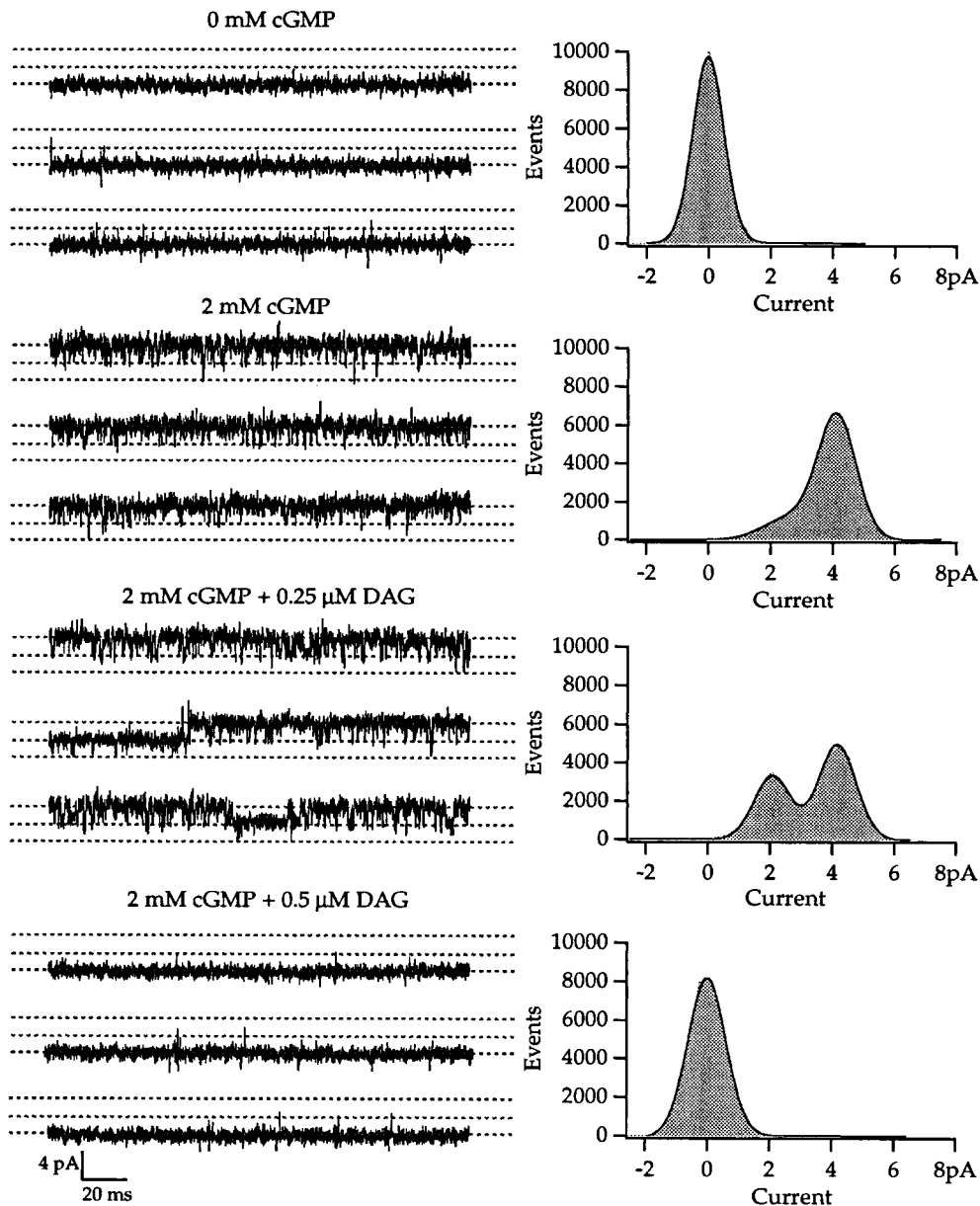
Rod Channel

FIGURE 4. DAG affects P_o rather than single-channel conductance of the rod channel. Currents recorded from an inside-out patch containing two α-homomultimeric mutant rod channels. These channels contained two point mutations (H468Q and A483V) that increased their cAMP efficacy to ~40%. However, like wild-type rod channels, they were very sensitively (IC$_{50}$ = 0.33 μM DAG) and fully inhibited by DAG even in the presence of saturating cGMP. Holding potential +80 mV, sampling rate 25 kHz after filtering at 5 kHz. Partial records are shown from five traces of 1 s duration. Patches were bathed in low divalent NaCl without cGMP, with saturating cGMP, and with two different DAG concentrations at saturating cGMP as designated. Amplitude histograms from full records (5 s) are shown to the right of each set of current traces. The histograms in the two middle panels were fit by the sum of two Gaussians, with means of 2.1 and 4.2 pA, suggesting a single-channel amplitude of 2.1 pA, with and without 0.25 μM DAG. The smooth lines represent the Gaussian fits, and the shaded areas indicate the histograms that were constructed from the data.

channel. In the presence of saturating cGMP, both rod and olfactory channels spent most of their time in the open state. With the addition of DAG to the bath, both types of channels spent more time closed. Furthermore, the single-channel amplitude remained unchanged by the DAG, at 2.1 pA for the rod channel and 3.2 pA for the olfactory channel. Thus, DAG causes a reduction in P_o, but does not appear to change the single-channel conductance.

DAG Inhibition Is Independent of Voltage

The addition of DAG at saturating cGMP alters the steady state current–voltage relations of both channels in a manner that reflects the lower P_o of each channel in the presence of DAG, suggesting that DAG does not impart its own voltage dependence but merely conveys the gating behavior that is apparent when fewer channels are open. In Fig. 6, the current–voltage relations for each channel are shown under three different experimental conditions: at saturating cGMP, both in the presence and absence of 2 μM DAG, as well as at a low cGMP concentration. For the rod channel, the addition of DAG at saturating cGMP creates a current–voltage relation similar to that observed when the channel responds to 10 μM cGMP, which is below the $K_{1/2}$ value for this patch. These relations show the characteristic increase in rectification seen for the native rod channel at low cGMP concentrations (Karpen et al., 1988). The

Olfactory Channel

0 mM cGMP

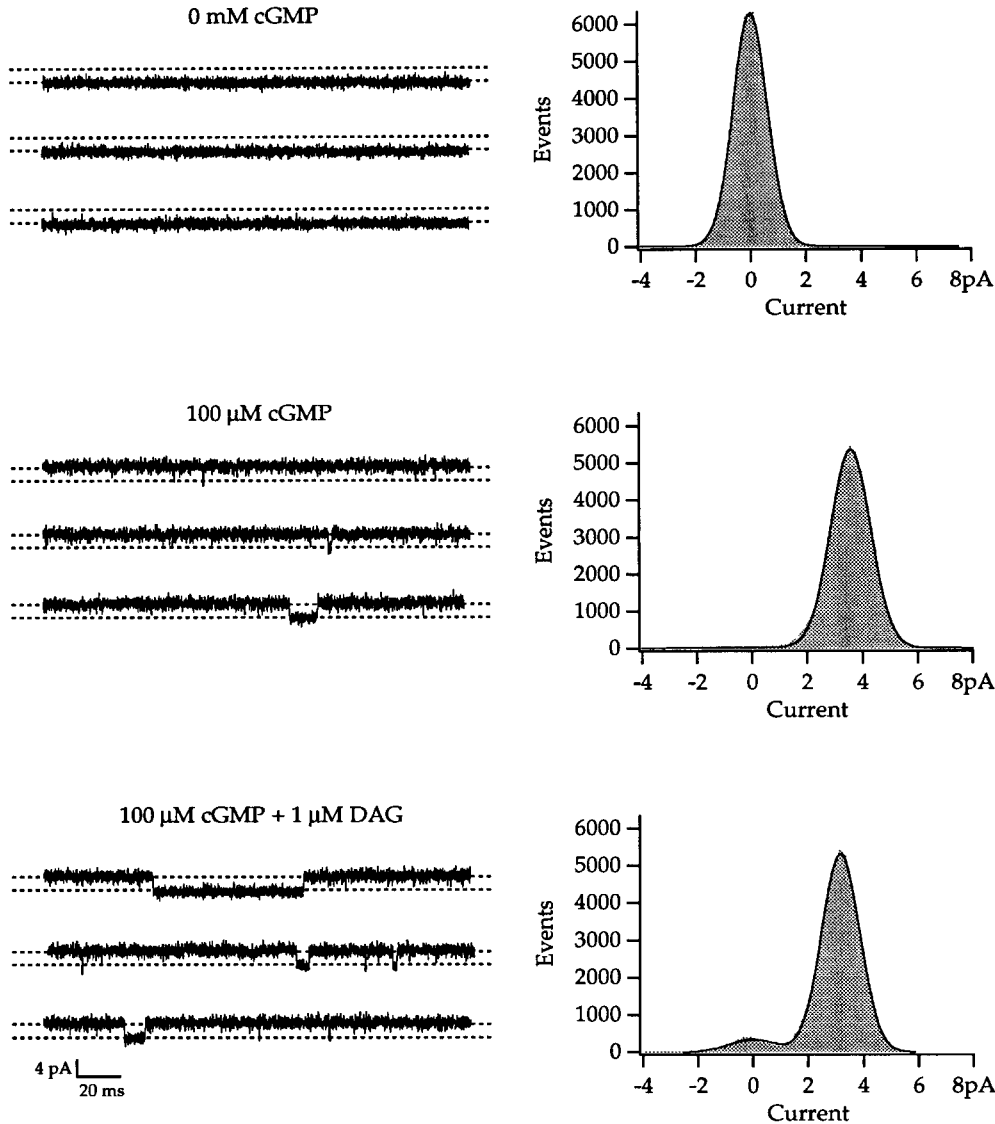### 100 μM cGMP

100 μM cGMP + 1 μM DAG

4 pA
20 ms

FIGURE 5. DAG affects P_o rather than single-channel conductance of the mouse olfactory channel. Currents were recorded and data are presented in the same manner as in Fig. 4; the patch contains a single olfactory channel. Partial records are shown from three traces of 1 s in length. Amplitude histograms from full records (3 s) are shown. The histograms were fit with Gaussians, indicating a mean single-channel current of 3.2 pA at +80 mV, with and without DAG.

current–voltage relation of the olfactory channel in the presence of 2 μM DAG at saturating cGMP correlates with the current–voltage relation observed when the channel responds to 5 μM cGMP, which is above the $K_{1/2}$ for this channel, reflecting the smaller effect of DAG on the olfactory channel. These current–voltage relations indicate that the only voltage dependence of DAG inhibition is that intrinsic to normal gating. This is in contrast to the voltage-dependent block observed with tetracaine (Fodor et al., 1997).

Structural Localization of Channel Region(s) Influencing Differential DAG Inhibition of Rod and Olfactory Channels

We used chimeras of rod and olfactory channels in an attempt to identify channel regions responsible for the differential inhibition of these two channels by DAG. For each chimera, we measured the $K_{1/2}$ for activation

by cGMP, the maximal percent inhibition by DAG at saturating cGMP and the DAG IC_{50} for this level of inhibition. Data were averaged from three to six patches for each chimera. Fig. 7 shows DAG dose–response curves measured at saturating cGMP for three representative chimeras, CHM3, CHM11, and CHM13 (see Fig. 8 for structures). Interestingly, although CHM3 contains the amino and carboxyl termini of the rod channel, its response to DAG is more like that of the olfactory channel; it is only partially inhibited by DAG and its IC_{50} (3.30 μM) is closer to that of the olfactory channel than to that of the rod channel. These data provided the first hint that the termini are not as important as the transmembrane segments and loops in determining the differential effects of DAG on rod and olfactory channels. Additional support for this notion comes from experiments with a mutant of the rod channel,
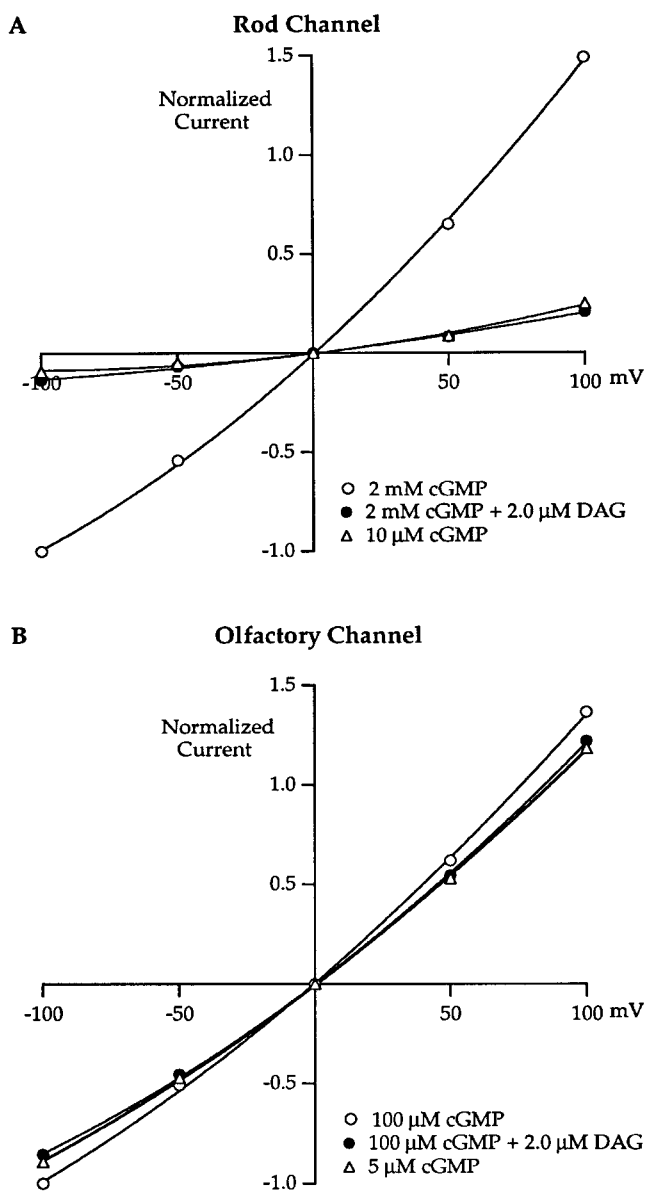
A

Rod Channel

Normalized Current

○ 2 mM cGMP
● 2 mM cGMP + 2.0 μM DAG
△ 10 μM cGMP

B

Olfactory Channel

Normalized Current

○ 100 μM cGMP
● 100 μM cGMP + 2.0 μM DAG
△ 5 μM cGMP

FIGURE 6. Inhibition by DAG is not voltage-dependent. Addition of DAG mimics a reduction in cGMP concentration, producing increased current–voltage rectification consistent with lower P_o. Steady state current–voltage relations constructed from data obtained from single patches; all data in a given plot are from the same patch. Open circles represent cGMP-activated currents at saturating cGMP in the absence of DAG. Closed circles represent currents at saturating cGMP in the presence of 2 μM DAG. For comparison, the triangles show the currents at lower cGMP concentration, without DAG: 10 μM cGMP for rod and 5 μM for olfactory. (A) Rod channels. (B) Olfactory channels.

H468Q. This mutant channel has dramatically increased cAMP efficacy (with saturating cAMP producing ∼40% of the maximal cGMP-activated current, as compared with only one to a few percent for wild-type rod channels). However, its DAG IC_{50} (0.33 μM, mean from 11 patches; data not shown) is not very different from that of the wild-type rod channel, and it is fully in-
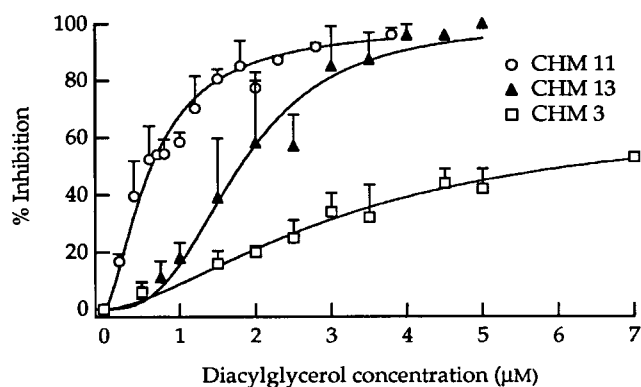

FIGURE 7. Examples of chimera channel behavior in response to DAG. This figure shows the amount of channel inhibition as a function of increasing DAG concentration for three chimeric constructs (structures depicted in Fig. 8). Points are mean values, plotted with SD (error bars). CHM 11: $IN_{max} = 100\%$, $IC_{50} = 0.63$ μM, and n = 1.6 (five patches). CHM 13: $IN_{max} = 100\%$, $IC_{50} = 1.80$ μM, and n = 2.8; (six patches). CHM 3: $IN_{max} = 68\%$, $IC_{50} = 3.30$ μM, and n = 1.6; 4 patches.

hibited by DAG at saturating cGMP. Thus, functionally significant mutations in the carboxyl terminus have rather insignificant effects on inhibition by DAG.

Fig. 8 shows the values of cGMP $K_{1/2}$ and of DAG IC_{50} at saturating cGMP for each chimera and the two wild-type channels. The results are displayed, along with the chimera structures, in the order of increasing cGMP $K_{1/2}$, which reflects the relative ease of opening of each chimera. Similar to the data for tetracaine inhibition observed by Fodor et al. (1997), the DAG IC_{50} and cGMP $K_{1/2}$ are roughly inversely correlated. However, this inverse correlation does not always strictly hold, as demonstrated in the companion paper (Crary et al., 2000, in this issue).

The corresponding maximum inhibition by DAG at saturating cGMP for each chimera and the wild-type channels is shown in Fig. 9, presented in the order of increasing maximum inhibition. The chimeras that reveal only partial inhibition tend to contain more olfactory-like sequences in the core regions of the channel, from S2 through S6 including the interconnecting loops of the transmembrane segments. In general, differences in the amino and carboxyl termini do not explain the differential DAG inhibition of the rod and olfactory channels; however, it appears that the presence of both amino and carboxyl termini from the rod in CHM3 may influence this chimera's behavior, increasing the maximum inhibition toward that of the rod channel.

DISCUSSION

Although extensive research has been performed on CNG channels, the molecular mechanism of gating is not fully understood. By exploring the molecular
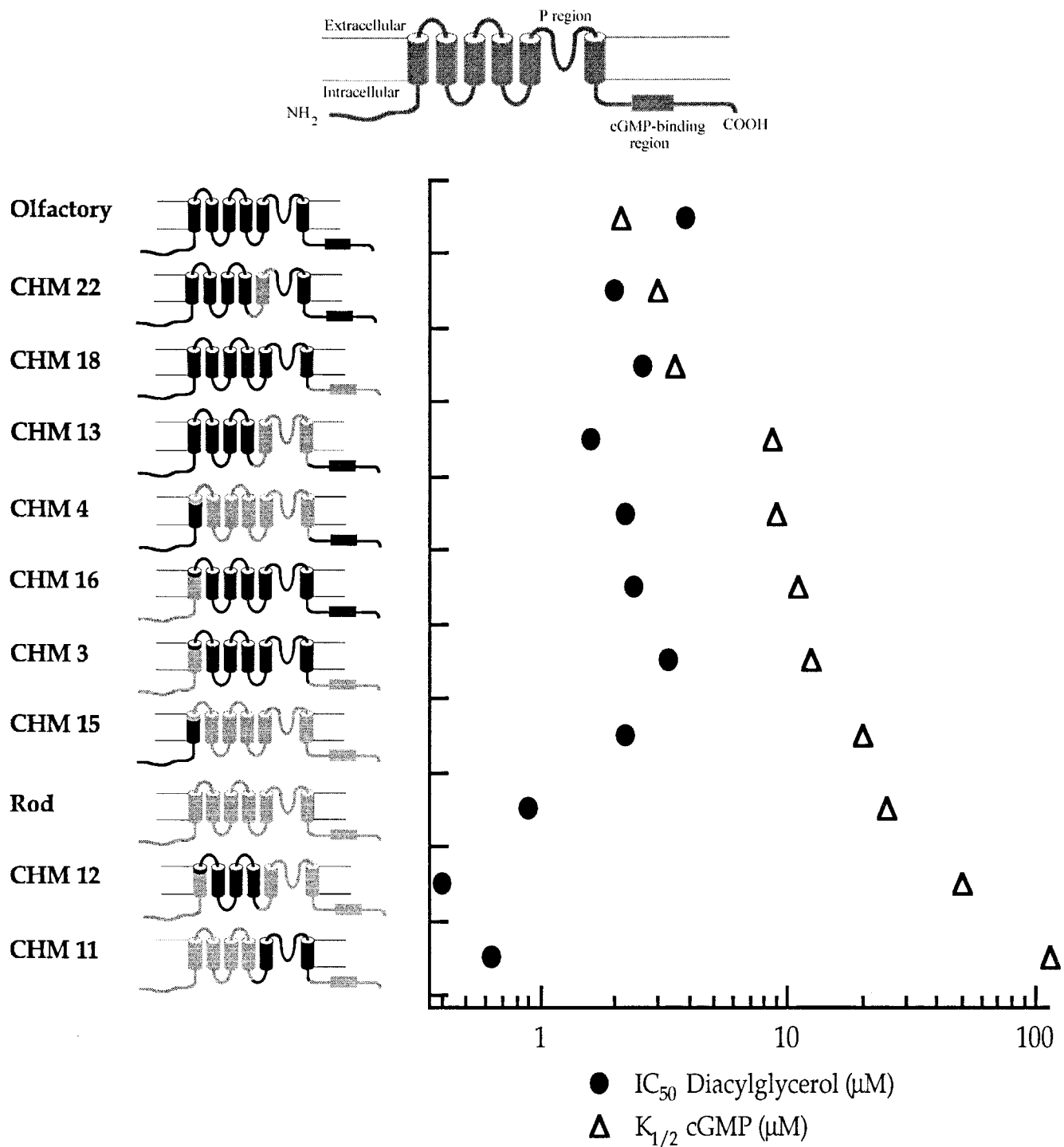
FIGURE 8. $K_{1/2}$ (cGMP) and IC_{50} (DAG) show an approximately inverse relationship among chimeras. In the chimera illustrations, the regions shown in black are from the olfactory channel, and the regions shown in gray are from the rod channel. A general channel diagram showing more detail is included at the top of the figure. The data for chimeras shown in this figure, but not included in Fig. 7, were measured from the following numbers of patches: CHM18 (six); CHM22 (six); CHM16 (five); CHM12 (three); CHM4 (five); and CHM15 (four). Chimeras are arranged from top to bottom in the order of increasing cGMP $K_{1/2}$ values. Points represent values of cGMP $K_{1/2}$ (triangles) and DAG IC_{50} (circles) obtained by fitting Hill curves to averaged data of each type (e.g., as in the cGMP dose–response curves without DAG shown in Fig. 2 and as in the DAG dose–response data at saturating cGMP shown in Figs. 3 and 7).
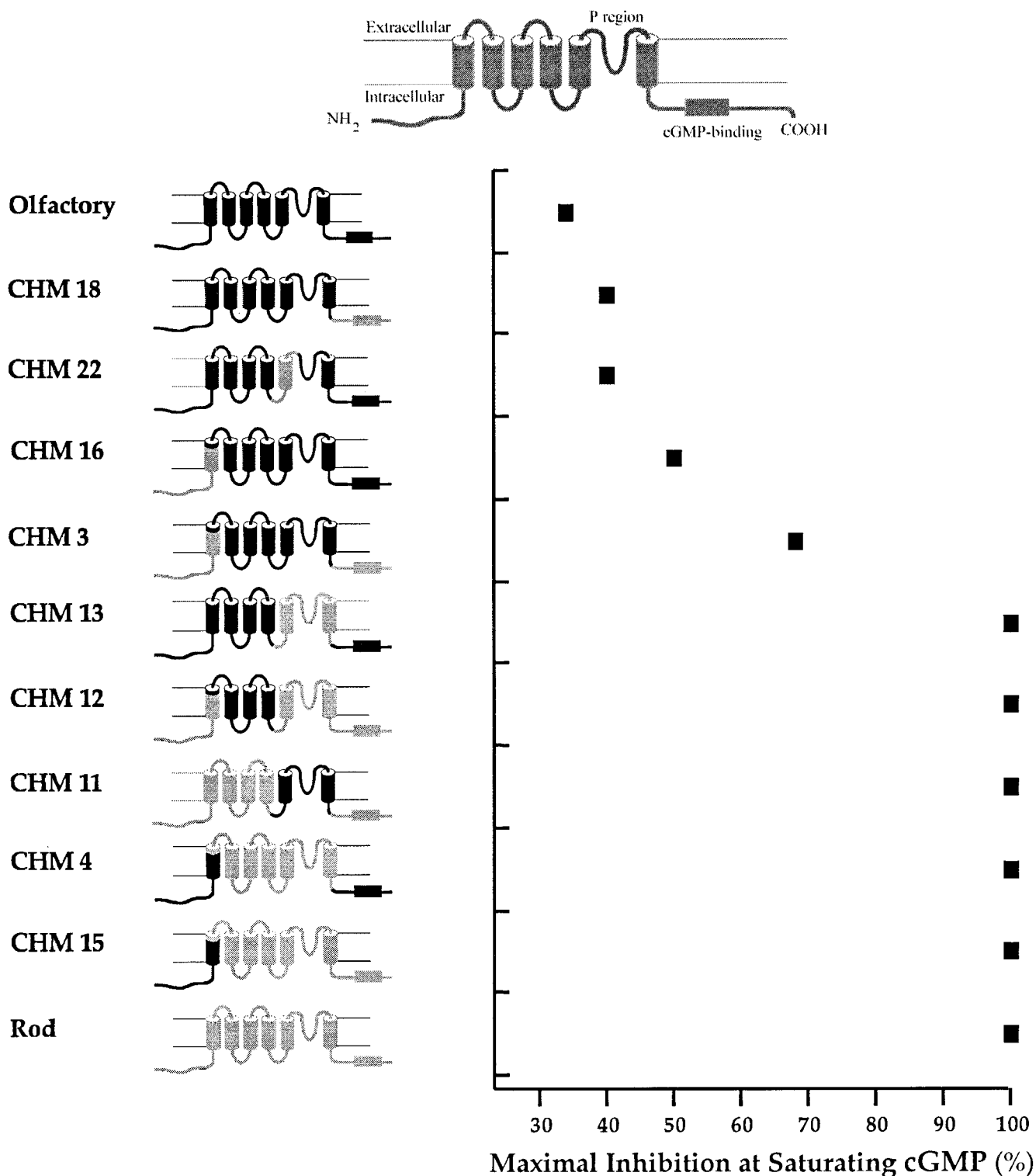
FIGURE 9. Maximal inhibition by DAG is greatest for chimeras whose transmembrane segments and loops are mostly of the rod channel type. Values for maximal inhibition were obtained from fits to the Hill equation while determining the IC_{50} values for Fig. 8.

mechanism of DAG inhibition of these channels, we may further understand the complex gating of these ion channels and, in particular, the differences between the properties of the rod and olfactory channels.

In this study, we have compared DAG inhibition of the bovine rod and rat olfactory α homomultimeric channels expressed in *Xenopus* oocytes. For both channels, inhibition by DAG is greater at low than at high chan-

nel P_o, indicating that DAG stabilizes the closed states of the channels (Figs. 1 and 3). This finding is consistent with that previously reported for DAG inhibition of the native CNG channel in amphibian rod cells (Gordon et al., 1995a). Single channel data (Figs. 4 and 5) support the notion that DAG inhibits the channels by lowering open probability. As before, the experiments were performed without the addition of ATP, indicating that the mechanism does not involve channel phosphorylation as a result of DAG activation of PKC. DAG inhibition of the cloned channels is also voltage-independent, with changes in current–voltage relations merely reflecting the lower P_o in the presence of DAG.

We find that rod CNG channels are much more strongly inhibited by DAG than are olfactory channels. This is especially apparent at saturating cGMP concentrations, where the rod cGMP-activated currents are completely abolished by DAG, but the olfactory currents are only partially suppressed even at high concentrations of DAG (Fig. 3). This finding suggests that the olfactory channel, whose opening is more energetically favored (Gordon and Zagotta, 1995b), is less sensitive to inhibition by DAG. This is reminiscent of the phenomenon observed for inhibition of these two channels by tetracaine (Fodor et al., 1997).

Our previous work with the native rod CNG channel suggested that DAG may be a closed state inhibitor (Gordon et al., 1995a). Here, we have more thoroughly addressed this question by comparing DAG inhibition of the rod and olfactory channels. In Figs. 1 and 2, the larger reduction in current at lower cGMP concentrations suggests that DAG stabilizes the closed or unliganded states of each channel. Furthermore, DAG has a much larger effect at saturating concentrations of the partial agonist (cAMP; data not shown) than at saturating cGMP, indicating that it is the P_o, rather than ligand occupancy, that matters. Fig. 3 provides further evidence that DAG is a closed state inhibitor. At low [cGMP], the DAG IC_{50} is decreased for both channels in comparison to the IC_{50} at saturating cGMP. In addition, the olfactory channel can be fully inhibited at low [cGMP] when the channels are more frequently in the closed state. Finally, Fig. 2 indicates that DAG is not a competitive inhibitor of cGMP binding, since large doses of cGMP cannot reverse the effects of DAG. These data are consistent with a mechanism in which DAG disturbs the allosteric opening transition of the channel.

To explore further the behavior of the channels in response to DAG, we also examined patches containing only one or two channels. Single-channel analysis revealed a DAG-induced decrease in P_o without a measurable change in single-channel conductance (Figs. 4 and 5). Hence, the reduction in the maximum current at saturating cGMP most likely was not due to the incom-

plete block of the pore by DAG, resulting in channel openings of lower current amplitude. The Hill coefficients from the DAG dose–response curves suggest that if DAG were to act by blocking the pore, it must do so with more than 1 molecule per channel. It appears that at least two DAG molecules are necessary for efficient inhibition of each channel (Fig. 3), raising the question of whether one DAG molecule interacts with each of the four channel subunits.

Since cloned rod and olfactory channels are differentially inhibited by DAG, we used a series of chimeras of these two channels in an attempt to attribute these differences in inhibition to specific regions of the channels. Chimeras have offered a valuable approach to understanding the differences in rod and olfactory channel behavior with respect to apparent agonist affinity, efficacy, and tetracaine inhibition (Goulding et al., 1994; Gordon and Zagotta, 1995b; Fodor et al., 1997). In this study, the series of chimeras from the Zagotta lab was examined with respect to cGMP $K_{1/2}$ (without DAG), DAG IC_{50} and maximal percent inhibition observed at saturating cGMP concentrations. From the chimera data, the core region of the channel seems to play a greater role in determining the differential DAG inhibition of the rod and olfactory channels than do the amino and carboxyl termini. Our chimera results demonstrate an approximately inverse relationship between cGMP $K_{1/2}$ and inhibitor IC_{50}, like that seen for inhibition by tetracaine (Fodor et al., 1997). However, we have recently found that a point mutation in the S2–S3 olfactory loop produces dramatic changes in DAG and tetracaine sensitivity with only minimal changes in apparent agonist affinity (Crary et al., 2000, in this issue).

Since PKC activation is not involved, DAG may have a direct inhibitory interaction with the CNG channels themselves or act on an unknown channel modulator that does not require the addition of nucleoside triphosphates. A previously defined DAG binding motif in protein kinase C and RasGRP contains repeats of histidine and cysteine residues (Ebinu et al., 1998). We could not identify such a consensus site in the primary sequence of the rod or olfactory CNG channel. However, the required residues for a consensus site may be present in distant parts of the primary sequence, and the repeat sequences may evolve upon folding. The DAG binding site could also be formed through coordination of residues from neighboring subunits of the tetramer, as proposed for the formation of a Ni^{2+} binding site through coordination of H420 from adjacent subunits in these channels (Gordon and Zagotta, 1995a,c). Alternatively, it is possible that CNG channels may have a binding site that differs from the documented consensus site.
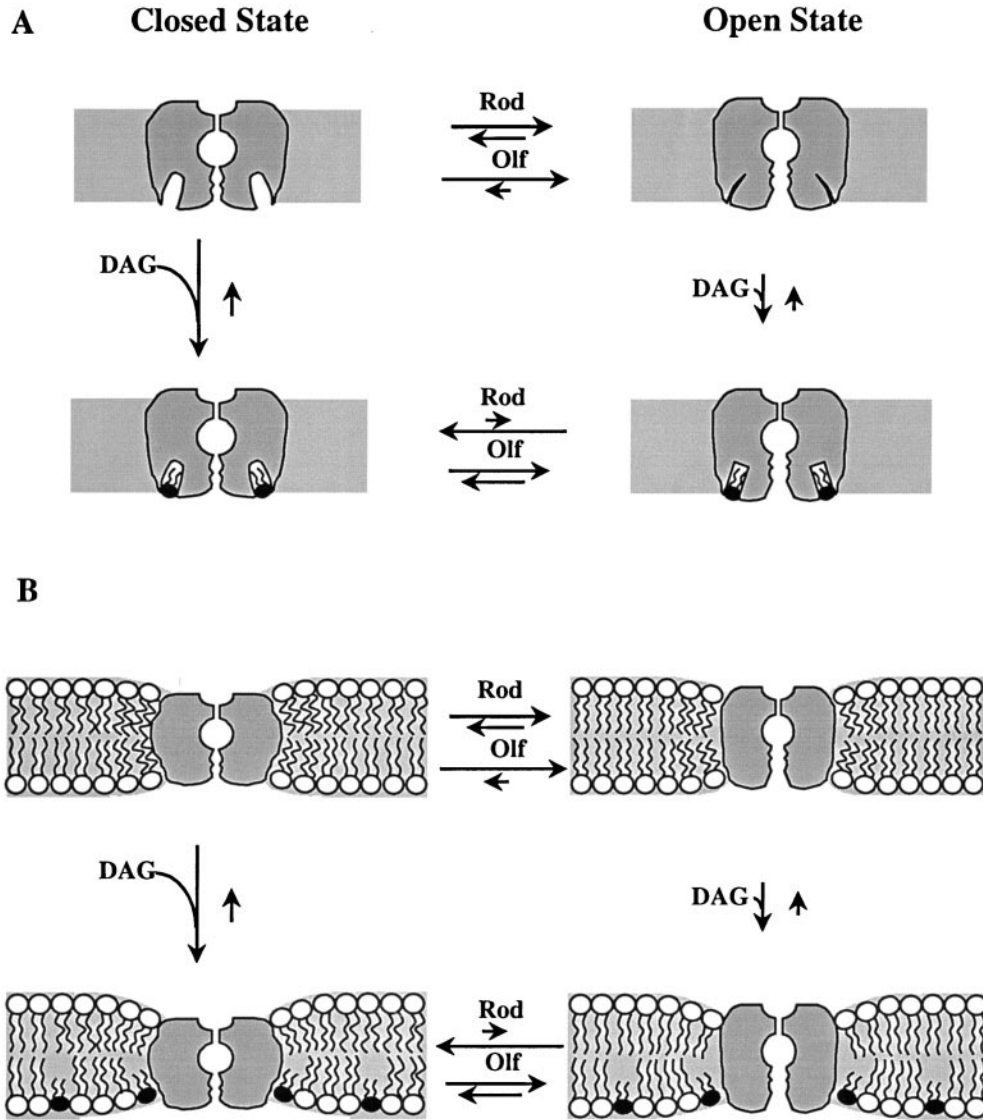
Our chimera study suggests that the transmembrane

A

Closed State   **Open State**

B

segments and attached loops may be important in determining the differential effects of DAG on rod and olfactory channels. Given the hydrophobic nature of DAG, the transmembrane segments are a likely target for this inhibitor. Furthermore, the spatial arrangement of the transmembrane segments may be critical for proper channel function. In other channels, rotation or twisting of these helical segments has been proposed for the allosteric transition from the closed to open state (Unwin, 1995; Perozo et al., 1999). Hence, DAG may act as a wedge that inserts into an intracellular crevice between adjacent transmembrane segments, thereby preventing pore expansion via movements of the core helices. Alternatively, once in place, the head group may interfere with the normal association of the intracellular loops, the amino terminus, or the carboxyl terminus with the membrane surface, which might occur during gating. The structure of the connecting loops may also be critical, providing flexibility or rigidity to attached transmembrane domains and possibly determining the overall structure of the channel. Future studies using chimeras and mutations involving

these regions may shed light on how DAG inhibits the conformational changes associated with the gating process and whether DAG, indeed, interacts directly with the channels.

In Fig. 10, we present two working models that represent possible mechanisms of DAG inhibition of olfactory and rod channels. Both models depict the two channels in either open or closed configurations (with and without DAG) at saturating agonist concentrations. The horizontal transitions in each model represent allosteric state changes, whereas vertical transitions represent binding or removal of multiple molecules of DAG. The top part of each diagram portrays the preference of both channel types for the open state in the absence of DAG, and the tendency for rod channels to be closed more of the time than are olfactory channels. For the rod channel, DAG strongly stabilizes the closed state, even under saturating agonist conditions. However, for the olfactory channel, the transition to the open state is still highly favored, even in the presence of DAG. This representation is based on the data showing that even high concentrations of DAG can only partially inhibit the olfactory channel at saturating [cGMP] (Fig. 3).

In the first model (Fig. 10 A), DAG is shown bound to a putative crevice on the intracellular side within the hydrophobic core of the channel. Alternatively, DAG may directly bind the channel at the hydrophobic interface between the transmembrane segments and the bilayer. An equally plausible mechanism (Fig. 10 B) for the action of DAG is that it inserts into the lipid bilayer, perturbing the coupling between the hydrophobic core of the bilayer and the hydrophobic membrane-spanning regions of the channel. This kind of alteration has been shown to modulate other channels (Lundbaek et al., 1996, 1997; Lundbaek and Andersen, 1999). For example, lysophospholipids have been shown to dramatically increase the dimerization constant for gramicidin (Lundbaek and Andersen, 1994). Interestingly, bilayer deformation effects can occur without changes in membrane fluidity, and can even show apparent cooperativity, with large Hill coefficients (Cantor, 1999), as observed with specific binding reactions (and as reported in this study).

The cartoon in Fig. 10 B shows one possible scenario by which DAG may alter bilayer–channel interactions. Here, the closed states are drawn distinctly shorter than the open states to suggest a smaller hydrophobic exterior surface of the protein. The surrounding bilayer is drawn with more curvature in the presence of DAG, to suggest a thinner, better matched, hydrophobic core at the interface between the bilayer and the closed channel. Thus, the addition of DAG is predicted to change the energetics of the channel conformational changes, thereby altering the open and closed probabilities. Of

course, DAG may regulate the channels by some combination of the mechanisms depicted in Fig. 10 (A and B). The actual physical changes that occur in channel gating remain to be determined, as does the detailed mechanism by which DAG alters the conformational equilibrium. However, it would seem that hydrophobic inhibitors such as DAG may prove useful in reporting intramolecular interactions and movements in the hydrophobic core of channels.

REFERENCES

Balasubramanian, S., J.W. Lynch, and P.H. Barry. 1996. Calcium-dependent modulation of the agonist affinity of the mammalian olfactory cyclic nucleotide-gated channel by calmodulin and a novel endogenous factor. *J. Membr. Biol.* 152:13–23.

Biel, M., W. Altenhofen, R. Hullin, J. Ludwig, M. Freichel, V. Flockerzi, N. Dascal, U.B. Kaupp, and F. Hofmann. 1993. Primary structure and functional expression of a cyclic nucleotide-gated channel from rabbit aorta. *FEBS Lett.* 329:134–138.

Biel, M., X. Zong, M. Distler, E. Bosse, N. Klugbauer, M. Murakami, V. Flockerzi, and F. Hofmann. 1994. Another member of the cyclic nucleotide-gated channel family, expressed in testis, kidney, and heart. *Proc. Natl. Acad. Sci. USA.* 91:3505–3509.

Bönigk, W., J. Bradley, F. Müller, F. Sesti, I. Boekhoff, G.V. Ronnett, U.B. Kaupp, and S. Frings. 1999. The native rat olfactory cyclic nucleotide-gated channel is composed of three distinct subunits. *J. Neurosci.* 19:5332–5347.

Bowlby, M.R., and I.B. Levitan. 1995. Block of cloned voltage-gated potassium channels by the second messenger diacylglycerol independent of protein kinase C. *J. Neurophysiology.* 73:2221–2229.

Broillet, M.C., and S. Firestein. 1999. Cyclic nucleotide-gated channels. Molecular mechanisms of activation. *Annu. NY Acad. Sci.* 868:730–740.

Cantor, R. 1999. Lipid composition and lateral pressure profile in bilayers. *Biophys. J.* 76:2625–2639.

Chen, T.-Y., and K.-W. Yau. 1994. Direct modulation by Ca^{2+}-calmodulin of cyclic nucleotide-activated channel of rat olfactory receptor neurons. *Nature.* 368:545–548.

Chyb, S., P. Raghu, and R.C. Hardie. 1999. Polyunsaturated fatty acids activate the *Drosophila* light-sensitive channels TRP and TRPL. *Nature.* 397:255–259.

Crary, J.I., D.M. Dean, F. Maroof, and A.L. Zimmerman. 2000. Mutation of a single residue in the S2-S3 loop of CNG channels alters the gating properties and sensitivity to inhibitors. *J. Gen. Phys.* 116:769–779.

Dionne, V.E., and A.E. Dubin. 1994. Transduction diversity in olfaction. *J. Exp. Biol.* 194:1–21.

Ebinu, J.O., D.A. Bottorf, E.Y.W. Chan, S.L. Stang, R.J. Dunn, and

J.C. Stone. 1998. RasGRP, a Ras guanyl nucleotide-releasing protein with calcium- and diacylglycerol-binding motifs. *Science.* 280:1082–1086.

Finn, J.T., M.E. Grunwald, and K.-W. Yau. 1996. Cyclic nucleotide-gated ion channels: an extended family with diverse functions. *Annu. Rev. Physiol.* 58:395–426.

Fodor, A.A., S.E. Gordon, and W.N. Zagotta. 1997. Mechanism of tetracaine block of cyclic nucleotide-gated channels. *J. Gen. Phys.* 109:3–14.

Gordon, S.E., and W.N. Zagotta. 1995a. A histidine residue associated with the gate of the cyclic nucleotide-activated channels in rod photoreceptors. *Neuron.* 14:177–183.

Gordon, S.E., and W.N. Zagotta. 1995b. Localization of regions affecting an allosteric transition in cyclic nucleotide-activated channels. *Neuron.* 14:857–864.

Gordon, S.E., and W.N. Zagotta. 1995c. Subunit interactions in co-ordination of Ni^{2+} in cyclic nucleotide-gated channels. *Proc. Natl. Acad. Sci. USA.* 92:10222–10226.

Gordon, S.E., D.L. Brautigan, and A.L. Zimmerman. 1992. Protein phosphatases modulate the apparent agonist affinity of the light-regulated ion channel in retinal rods. *Neuron.* 9:739–748.

Gordon, S.E., J. Downing-Park, B. Tam, and A.L. Zimmerman. 1995a. Diacylglycerol analogs inhibit the rod cGMP-gated channel by a phosphorylation-independent mechanism. *Biophys. J.* 69:409–417.

Gordon, S.E., J. Downing-Park, and A.L. Zimmerman. 1995b. Modulation of the cGMP-gated ion channel in frog rods by calmodulin and an endogenous inhibitory factor. *J. Physiol.* 486:533–546.

Goulding, E.H., G.R. Tibbs, and S.A. Siegelbaum. 1994. Molecular mechanism of cyclic-nucleotide-gated channel activation. *Nature.* 372:369–374.

Hofmann, T., A.G. Obukhov, M. Schaefer, C. Harteneck, T. Gudermann, and G. Schultz. 1999. Direct activation of human TRPC6 and TRPC3 channels by diacylglycerol. *Nature.* 397:259–263.

Hsu, Y.-T., and R.S. Molday. 1993. Modulation of the cGMP-gated channel of rod photoreceptor cells by calmodulin. *Nature.* 361:76–79.

Idelfonse, M., S. Crouzy, and N. Bennett. 1992. Gating of retinal rod cation channel by different nucleotides: comparative study of unitary currents. *J. Membr. Biol.* 130:91–104.

Jan, L.Y., and Y.N. Jan. 1992. Tracing the roots of ion channels. *Cell.* 69:715–718.

Karpen, J.W., A.L. Zimmerman, L. Stryer, and D.A. Baylor. 1988. Gating kinetics of the cyclic-GMP-activated channel of retinal rods: flash photolysis and voltage-jump studies. *Proc. Natl. Acad. Sci. USA.* 85:1287–1291.

Karpen, J.W., R.L. Brown, L. Stryer, and D.A. Baylor. 1993. Interactions between divalent cations and the gating machinery of cyclic GMP-activated channels in salamander retinal rods. *J. Gen. Phys.* 101:1–25.

Kaupp, U.B. 1995. Family of cyclic nucleotide gated ion channels. *Curr. Opin. Neurobiol.* 5:434–442.

Liman, E.R., J. Tytgat, and P. Hess. 1992. Subunit stoichiometry of a mammalian K^+ channel determined by construction of multimeric cDNAs. *Neuron.* 9:861–871.

Lundbaek, J.A., and O.S. Andersen. 1994. Lysophospholipids modulate channel function by altering the mechanical properties of lipid bilayers. *J. Gen. Phys.* 104:645–673.

Lundbaek, J.A., and O.S. Andersen. 1999. Spring constraints for gramicidin-induced lipid bilayer deformations estimates using gramicidin channels. *Biophys. J.* 76:889–895.

Lundbaek, J.A., P. Birn, J. Girshman, A.J. Hansen, and O.S. Andersen. 1996. Membrane stiffness and channel function. *Biochemistry.* 35:3825–3830.

Lundbaek, J.A., A.M. Maer, and O.S. Andersen. 1997. Lipid bilayer electrostatic energy, curvature stress, and assembly of gramicidin channels. *Biochemistry.* 36:5695–5701.

Marsh, D., and D. Phil. 1990. CRC Handbook of Lipid Bilayers. CRC Press, Boston. 276.

Menini, A. 1995. Cyclic nucleotide-gated channels in visual and olfactory signal transduction. *Biophys. Chem.* 55:185–196.

Molday, R.S., and Y.-T. Hsu. 1995. The cGMP-gated channel of photoreceptor cells: its structural properties and role in phototransduction. *Behav. Brain Sci.* 18:441–451.

Molokanova, E., B. Trivedi, A. Savchenko, and R.H. Kramer. 1997. Modulation of rod photoreceptor cyclic nucleotide-gated channels by tyrosine phosphorylation. *J. Neurosci.* 17:9068–9076.

Muller, F., W. Bönigk, F. Sesti, and S. Frings. 1998. Phosphorylation of mammalian olfactory cyclic nucleotide-gated channels increases ligand sensitivity. *J. Neurosci.* 18:164–173.

Perozo, E., D.M. Cortes, and L.G. Cuello. 1999. Structural rearrangements underlying K^+-channel activation gating. *Science.* 285:59–61.

Richards, M.J., and S.E. Gordon. 2000. Cooperativity and cooperation in cyclic nucleotide-gated ion channels. *Biochemistry.* In press.

Roof, D.J., and C.L. Makino. 2000. The structure and function of retinal photoreceptors. *In* The Principals and Practice of Ophthalmology. Volume 3. D.M. Alberts and F.A Jakobiec, editors. W.B. Saunders, Philadelphia. 1624–1673.

Ruiz, M.L., B. London, and B. Nadal-Ginard. 1996. Cloning and characterization of an olfactory cyclic nucleotide-gated channel expressed in mouse heart. *J. Mol. Cardiol.* 28:1453–1461.

Unwin, N. 1995. Acetylcholine receptor channel imaged in the open state. *Nature.* 373:37–43.

Wei, J.-Y., D.S. Roy, L. Leconte, and C.J. Barnstable. 1998. Molecular and pharmacological analysis of cyclic nucleotide-gated channel function in the central nervous system. *Progr. Neurobiol.* 56:37–64.

Womack, K.B., S.E. Gordon, F. He, T.G. Wensel, C.C. Lu, and D.W. Hilgemann. 2000. Do phosphatidylinositides modulate vertebrate phototransduction? *J. Neurosci.* 20:2792–2799.

Yau, K.-W., and T.Y. Chen. 1995. Cyclic nucleotide-gated channels. *In* Handbook of Receptors and Channels: Ligand and Voltage-gated Ion Channels. R.A. North, editor. CRC Press, Boca Raton, FL. 307–335.

Zagotta, W.N., and S.A. Siegelbaum. 1996. Structure and function of cyclic nucleotide-gated channels. *Annu. Rev. Neurosci.* 19:235–263.

Zimmerman, A.L. 1995. Cyclic nucleotide gated ion channels. *Curr. Opin. Neurobiol.* 5:296–303.

Zimmerman, A.L., and D.A. Baylor. 1992. Cation interactions within the cyclic GMP-activated channel of retinal rods from the tiger salamander. *J. Physiol.* 449:759–783.

Zimmermann, A., P. Gehr, and H.U. Keller. 1988. Diacylglycerol-induced shape changes, movements and altered F-actin distribution in human neutrophils. *J. Cell Sci.* 90:657–666.

Zufall, F., S. Firestein, and G.M. Sheperd. 1994. Cyclic nucleotide-gated ion channels and sensory transduction in olfactory receptor neurons. *Annu. Rev. Biophys. Biomol. Struct.* 23:577–607.